Available online at www.sciencedirect.com
SCIENCE DIRECT®
Biomaterials 24 (2003) 2821–2829
Biomaterials
www.elsevier.com/locate/biomaterials

Activation of platelets adhered on amorphous hydrogenated carbon (a-C:H) films synthesized by plasma immersion ion implantation-deposition (PIII-D)

P. Yang[a,b], N. Huang[b], Y.X. Leng[b], J.Y. Chen[b], R.K.Y. Fu[a], S.C.H. Kwok[a], Y. Leng[c], P.K. Chu[a,*]

[a] *Department of Physics and Materials Science, City University of Hong Kong, 83 Tat Chee Avenue, Kowloon, Hong Kong, China*
[b] *School of Materials Science & Engineering, Southwest Jiaotong University, Chengdu 610031, China*
[c] *Department of Mechanical Engineering, Hong Kong University of Science & Technology, Clear Water Bay, Kowloon, Hong Kong, China*

Received 12 July 2002; accepted 29 January 2003

Abstract

Amorphous carbon films have attracted much attention recently due to their good biocompatibility. Diamond-like carbon (DLC), one form of amorphous carbon that is widely used in many kinds of industries, has been proposed for use in blood contacting medical devices. However, the blood coagulation mechanism on DLC in a biological environment is not well understood. Platelet adhesion and activation are crucial events in the interactions between blood and the materials as they influence the subsequent formation of thrombus. In this work, the behavior of platelets adhered onto hydrogenated amorphous carbon films (a-C:H) is investigated. Hydrogenated amorphous carbon films with different hydrogen contents, structures, and chemical bonds were fabricated at room temperature using plasma immersion ion implantation-deposition (PIII-D). The wettability of the films was investigated by contact angle measurements using several common liquids. Platelet adhesion experiments were conducted to examine the interaction of blood with the films in vitro and the activation of adherent platelets. The results show that the behavior of the platelets adhered on the a-C:H films is influenced by their structure and chemical bond, and it appears that protein interaction plays a key role in the activation of the adherent platelets.

Keywords: Hydrogenated amorphous carbon (a-C:H) film; Haemocompatibility; Platelet activation; Plasma immersion ion implantation-deposition (PIII-D)

1. Introduction

The usual failure of blood-contacting biomedical materials and devices arises from thrombogenesis and it has prompted researchers to develop new materials and improve the fabrication processes. Diamond-like carbon (DLC) films have been studied extensively and used in industry due to their excellent properties such as extremely high hardness, high density, low friction coefficient, chemical inertness, relatively high thermal conductivity, and visual transparency. Recently, DLC has been proposed for use in blood-contacting devices [1–3] such as rotary blood pumps [4,5], artificial hearts [6], mechanical heart valves [7–9], and coronary artery stents [10,11]. However, the blood coagulation mechanism on DLC films in a biological environment is not well understood and there have only been a few reports on this topic [2,8,12,13]. Some results have shown that cell adhesion onto DLC coatings is related to the bonding structure (i.e. fraction of sp^3 bonds) [13,14], surface energy and hydrophobicity [8,12], smooth surface [14], and film thickness [5].

Whenever a foreign surface is placed in contact with blood, an interface forms between the materials surface and blood. Plasma protein adsorption is the initial event in the blood–materials interaction and influences subsequent platelet adhesion and activation [15–19]. These events then lead to blood clotting when activated platelets secrete substances that enzymatically activate otherwise inactive clotting factors, culminating in the

*Corresponding author. Tel.: +852-27887724; fax: +852-27889549 or +852-27887830.
E-mail address: paul.chu@cityu.edu.hk (P.K. Chu).

0142-9612/03/$ - see front matter
doi:10.1016/S0142-9612(03)00091-7

formation of an insoluble mesh of fibrin polymer. Thus, platelet adhesion and activation are crucial events in blood–materials interaction as they influence the subsequent formation of thrombus. We report here our investigation of the behavior of platelets adhered onto hydrogenated amorphous carbon films (a-C:H) and the activation mechanism.

2. Materials and methods

Hydrogenated amorphous carbon films were fabricated at room temperature using plasma immersion ion implantation-deposition (PIII-D) [20]. Silicon wafers (1 0 0) were used as substrates. Prior to film deposition, the substrates underwent Ar^+ sputter cleaning for 15 min at a base pressure of about 2×10^{-3} Pa to remove surface contaminants and surface oxide using a radio frequency (RF) power of 500 W and a substrate DC bias voltage of −500 V. A mixture of acetylene (C_2H_2) and argon was subsequently introduced into the chamber and the plasma was triggered using RF. Film deposition was carried out at a constant RF power of 500 W. During the initial deposition of the base film, a higher negative DC bias voltage was applied to the sample holder to improve film adhesion by means of ion mixing. A series of DLC films were synthesized by adjusting the substrate bias voltage in subsequent deposition of the top films. The PIII-D process time was 2 h and the detailed deposition parameters are listed in Table 1. The film thickness was measured with an Alpha-step®-500 surface profiler.

Structural information of the films was obtained by a Renishaw RM 3000 Micro-Raman system at room temperature using a 25 mW He–Ne laser (633 nm). Graphite was used as the control in the analysis. Fourier transform infrared spectroscopy (FTIR) was employed to evaluate the C–H bonding state in the DLC films. The transmission spectra were taken between 400 and 4000 cm^{-1} with a resolution of 2 cm^{-1}. The film composition was measured by Rutherford backscattering spectrometry (RBS) and X-ray photoelectron spectroscopy (XPS).

The surface properties of the films were investigated. Wettability examinations were performed using the sessile drop method using a JY-82 contact angle goniometer. The test liquids used in the tests are listed in Table 2 together with their relative surface tension components. Contact angle measurements were measured using at least four drops of each liquid for each sample in order to get good statistical averages.

As reported in the literature, the work of adhesion (W_a) between a liquid and a solid was given by the Young [21] equation (Eq. (1)) and the Van Oss [22] equation (Eq. (2)):

$$W_a = \gamma_l(1+\cos\theta), \tag{1}$$

$$W_a = (\gamma_l^p\gamma_s^p)^{1/2} + (\gamma_l^d\gamma_s^d)^{1/2}, \tag{2}$$

where θ is the contact angle, γ_l, γ_l^d and γ_l^p are the surface tension and its polar and dispersive components of the liquid phases, respectively, and γ_s^p and γ_s^p are the polar and dispersive components of the solid phases.

From Eqs. (1) and (2), we obtain

$$(\gamma_l^p\gamma_s^p)^{1/2} + (\gamma_l^d\gamma_s^d)^{1/2} = \gamma_l(1+\cos\theta). \tag{3}$$

Consequently, measurements with only two different liquids with known polar and dispersive components are needed to solve Eq. (3). Thus, the polar and dispersive components of the investigated coatings were determined by a contact angle measurement using six different liquids.

Platelet adhesion experiments were conducted to evaluate the surface thrombogenicity of the films and to examine the interaction between blood and the materials in vitro. All the a-C:H films were cleaned and then incubated in human platelet rich plasma (PRP) for 15 min at 37°C. After rinsing, fixing, and critical point

Table 2
Surface tension and surface tension components of liquids used in contact angle test (mJ/m^2)

Liquid	γ_l	γ_l^d	γ_l^p
Water	72.8	21.8	51.0
Glycerin	63.4	37	26.4
Formamide	58.2	39.5	18.7
Diiodomethane	50.8	48.5	2.3
Glycol	48.3	29.3	19
Tritolyl phosphate	40.9	39.2	1.7

Table 1
Synthesis parameters of the DLC films

Sample identification		a-C:H-1	a-C:H-2		a-C:H-3	a-C:H-4
Working pressure (10^{-1} Pa)		1.30	1.22		1.21	1.22
C_2H_2 flow				10		
Flow ratio (C_2H_2/Ar)				1/2		
Base layer deposition	Bias voltage (V)			−900		
	Time (min)			30		
Outer layer deposition	Bias voltage (V)	−75	−150		−300	−900
	Time (min)	90	90		90	90
Thickness (nm)		310	270		90	70

drying, the specimens were examined using scanning electron microscopy (SEM) and optical microscopy. The quantity and morphology of the adherent platelets were investigated to assess platelet adhesion and activation employing the point counting method at a magnification factor of 1000. Ten fields were chosen at random to obtain statistical averages of the adherent platelets. Low temperature isotropic carbon (LTI-carbon) and stainless steel are commonly used as the blood-contacting biomaterials. Compared with stainless steel, LTI-carbon is the preferred material for mechanical heart valve prostheses due to its better blood-compatibility. In the work reported here, LTI-carbon and stainless steel were used as positive or negative controls, respectively.

The morphological change of the adherent platelets is a common qualitative criterion to assess activation of adherent platelet on the materials surface. The unactivated platelets typically manifest as disc-shaped cells about 2–3 μm in size. Slight pseudopodia indicate the early stage of activation. A different morphology exhibiting heavily developed pseudopodia, larger size (> 5 μm), and more depressed shape indicates a high state of activation.

3. Results and discussion

3.1. Film characteristics

The Raman spectra acquired from the hydrogenated DLC (a-C:H) films are exhibited in Fig. 1. Compared with graphite, all the spectra show a broad peak at around 1550 cm^{-1} and a lower frequency shoulder. They can be fitted employing two Gaussian peaks at about 1550 and 1350 cm^{-1}, which correspond to the G and D lines of graphite, respectively [23]. Based on the fitting parameters, the peak position and the ratio of the integrated areas under the G and D peaks (I_D/I_G) are obtained and summarized in Table 3 . Our results show that a higher bias voltage (V_b) leads to shifts of the two peaks towards higher wave numbers and increasing I_D/I_G ratios. The positions of the G and D lines, G-full width at half-maximum and integrated intensity ratio (I_D/I_G) can be correlated with the sp^3/sp^2 bonding ratio [24], graphite cluster size [25,26], and disorder in these threefold coordinated islands [27]. Hence, the sp^3/sp^2 ratios in the a-C:H films cannot be derived directly from the Raman spectra, but nevertheless, some qualitative information can be extracted. Increases in the I_D/I_G ratio, shifting of the G-peak towards higher wave numbers, widening of the D-peak, and narrowing of the G-peak are caused by increase of the graphite-like component in the amorphous carbon films [28]. Our

Table 3
Experimental results derived from Raman spectroscopy

Sample	Peak position (cm^{-1})[a]		I_D/I_G[b]
	G-band	D-band	
a-C:H-1	1536	1350	1.51
a-C:H-2	1537	1354	1.52
a-C:H-3	1549	1362	2.30
a-C:H-4	1563	1371	3.30

[a] Full-width half-maximum.
[b] Intensity ratio of D-band to G-band.

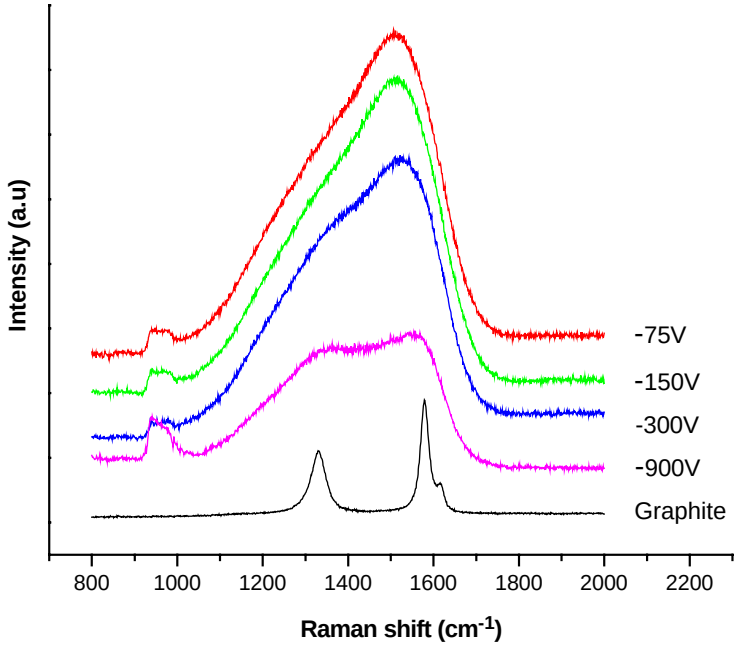

Fig. 1. Raman spectra of the a-C:H films fabricated at different bias voltages.

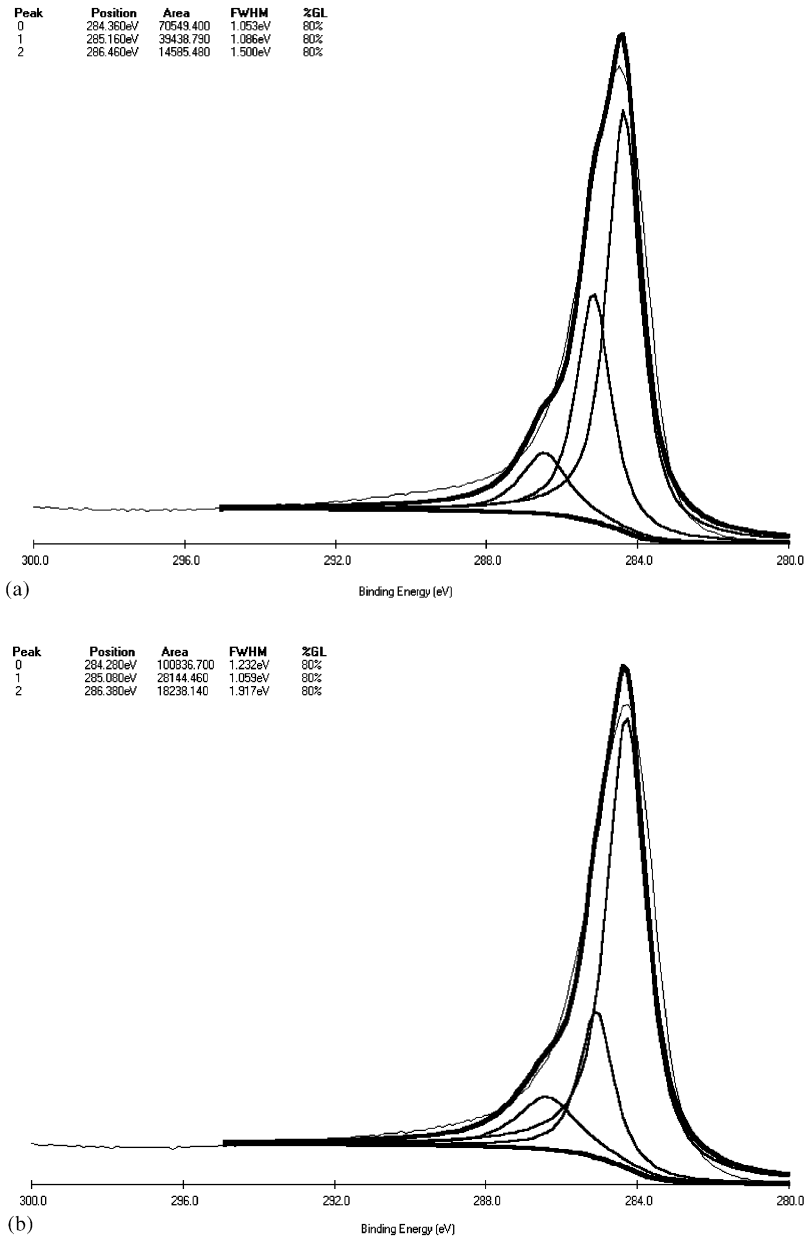

Fig. 2. Comparison of C 1s XPS spectra of the a-C:H films deposited at: (a) −75 V and (b) −900 V.

results indicate that the film structure becomes more graphite like with increasing substrate bias. One of the reasons is that the increase in substrate temperature induced by higher energetic ion bombardment promotes film graphitization, as it has been shown that such a graphitization process is thermally driven [29].

Fig. 2 shows the XPS spectra of C (1s) acquired from the samples after 8 min of sputtering to remove surface contaminants. Compared to the spectrum of film deposited at −75 V DC bias, the C 1s peak of the −900 V sample shifts to a lower binding energy of 284.2 eV. The corresponding C 1s spectra can be deconvoluted into three peaks situated at approximately 284.3, 285.1 and 286.4 eV. It is known that the C 1s peak of graphite is at 284.0–284.5 eV, for diamond at 285.0–285.2 eV, for C–H at 284.9–285.5 eV, and for C–O at 286.4–286.8 eV [30–32]. Obviously, it is difficult to determine the sp^3/sp^2 ratio quantitatively based on the XPS results alone because we cannot separate the sp^3 C–C and C–H bonds. However, when V_b is changed from −75 to −900 V, the $sp^2/(sp^3 + C–H)$ ratio increases from 1.8 to 3.6, and it is clear that the film deposited at −900 V is more graphite like.

Fig. 3 shows the RBS spectra of the DLC films. The C concentration is quite uniform with depth in all the samples, and the films deposited using a larger bias are thinner, thereby corroborating our profilometry results. A trace amount of argon from the plasma is observed in

the films as indicated by the RBS data. The areal densities (atoms/cm^2) of carbon in the a-C:H films calculated from the RBS results are listed in Table 4, showing higher areal carbon densities with decreasing sample bias V_b, indicating that the sp^3 content of the films also increases with decreasing absolute value of V_b.

FTIR can more easily discern C–H sp^2 and sp^3 bonds, and the FTIR spectra obtained from the DLC films prepared at different substrate DC bias voltages are displayed in Fig. 4. Similar to reports in the literature [33–35], no fine structures are observed from the C–H absorption spectra from 2500 to 3500 cm^{-1}. Hence, it can be inferred that the atomic hydrogen in the films is free and not bonded to carbon.

3.2. Surface energy and wettability

The surface energy (γ_s) and its polar and dispersive components (γ_s^p and γ_s^d) calculated from the linear fitting curves of Eq. (3) are shown in Fig. 5 together with the contact angle of water. The results show that all the surfaces have a hydrophobic nature with much higher γ_s^d than γ_s^p. As the absolute value of the bias voltage increases, the polar part of the surface energy decreases by nearly 60% from 6.4 to 3.8 mJ/m^2. The contact angle of water for the films is about 75–85° and decreases with higher V_b. The trends are consistent with the change of the I_D/I_G ratio (Fig. 6). The surface energy thus appears to be affected mainly by the sp^3 content in the films, and Pinzari's study on the wettability of diamond films in fact showed similar effects [36].

3.3. Platelet adhesion and activation

Fig. 7 exhibits the statistical results of the platelets adhered on the a-C:H film surfaces from PRP, expressed as a percentage of platelets adhered on the stainless steel in the same test. After incubation in PRP for 15 min, the number of adherent platelets slightly decreases with increasing V_b (absolute value) and is less than that on stainless-steel surface. The percentage of un-activated platelets drops steeply from 30% to 8% when V_b is changed from −75 to −900 V. The percentage of un-activated platelets on stainless steel is in between.

The morphology of the adherent platelets observed by SEM is displayed in Fig. 8. As shown in Fig. 8a, the adherent platelets on the surface of the film deposited at −75 V are isolated and nearly round, while slight pseudopodium occurs. The haemocompatibility of this film is better than that of stainless steel (Fig. 8d) and similar to that of LTI-carbon (Fig. 8e). In comparison, most of the adherent platelets on the surface of film deposited at −900 V are in a spreading pseudopodium state. They interconnect to each other and form aggregation. It is also observed that the adherent

Table 4
Calculated areal density of carbon-atoms in the a-C:H films from RBS

Sample	C density (10^{15} atoms/cm^2)
a-C:H-1	798
a-C:H-2	541.5
a-C:H-4	223.2

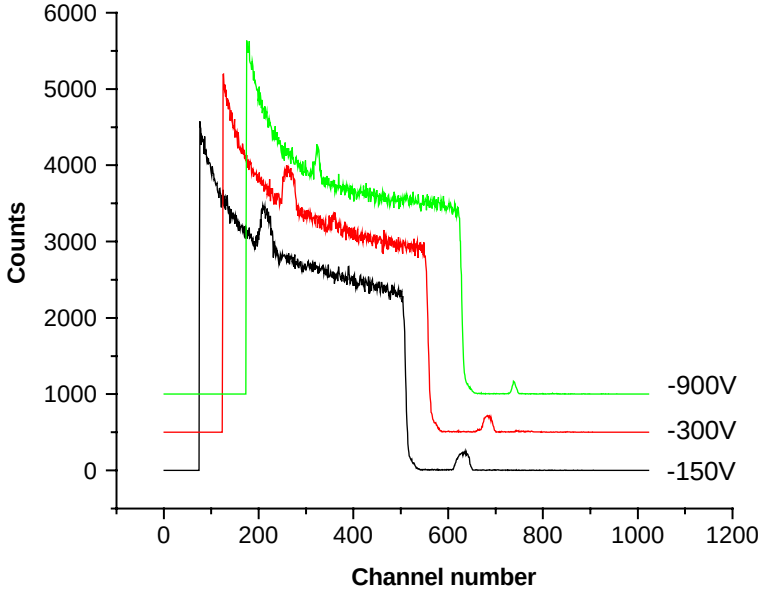

Fig. 3. RBS spectra obtained from the a-C:H films fabricated at various bias voltages.

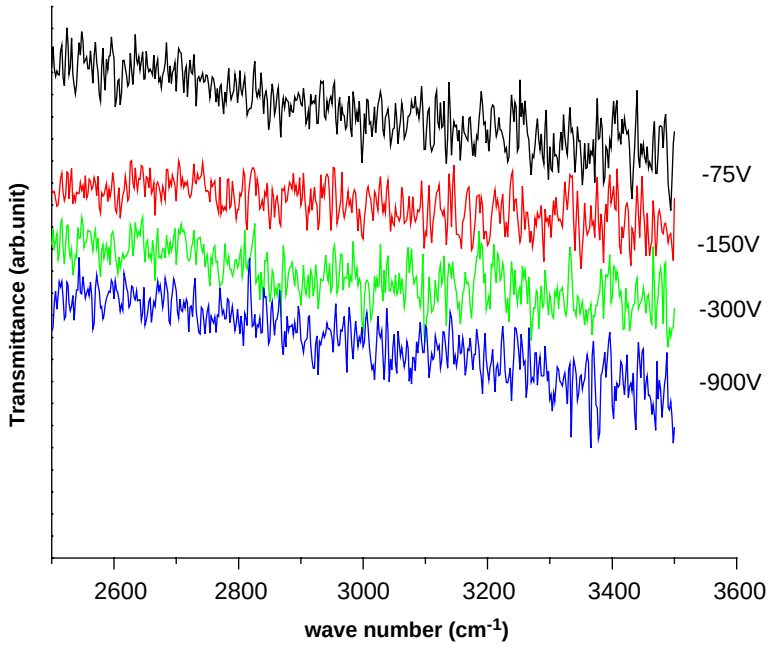

Fig. 4. FTIR spectrum of the a-C:H films fabricated at different bias voltages.

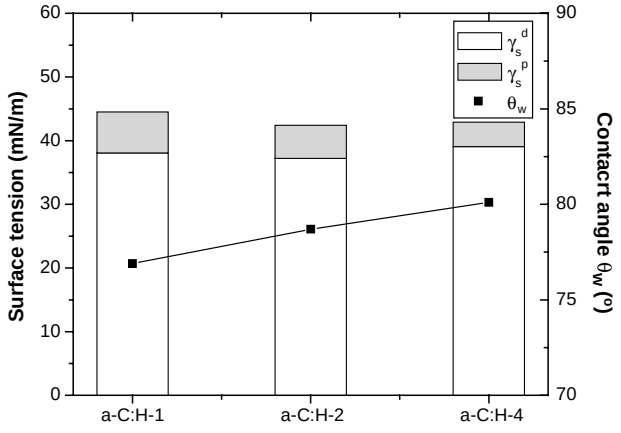

Fig. 5. Surface energies (γ_s) and their polar and dispersive components (γ_s^p and γ_s^d) of the a-C:H films.

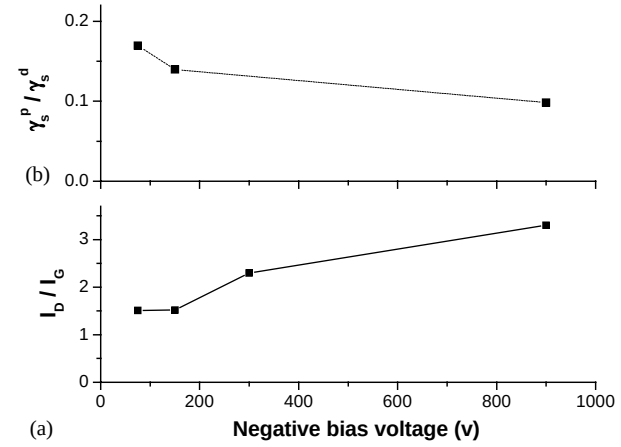

Fig. 6. Effects of the bias voltage on: (a) Intensity ratio of the D-band to G-band and (b) Ratio of polar/dispersive component of the surface energy.

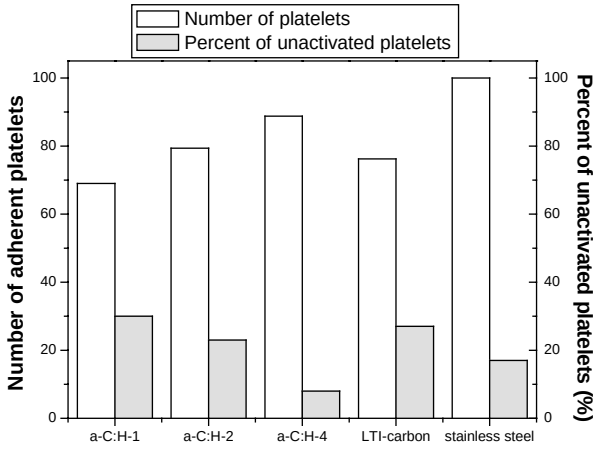

Fig. 7. Quantity of platelets adhered on the surface of the a-C:H films synthesized at different bias voltages (15 min incubation in PRP) (Expressed as a percentage of platelets adhering on the stainless steel in the same test).

platelets in the bottom zone are in a higher degree of spreading (Fig. 8c). Platelet activation on the surface of a material can be assessed by their degree of spreading and changing shape [12,37]. Thus, platelets are strongly surface activated by the a-C:H film deposited at high V_b (absolute value) compared to those at low V_b (absolute value). It is consistent with the variation of the polar component γ_s^p of the surface energy. The platelet attachment and morphology studies suggest that the adhesion behavior of the platelets is related to the surface energy of the film. The higher the absolute value of V_b, the lower is the value of γ_s^p, and accordingly, the higher the activation of adherent platelets.

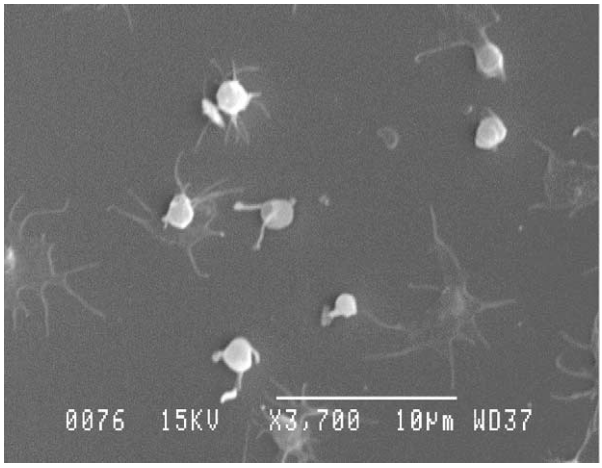

(a) a-C:H-1

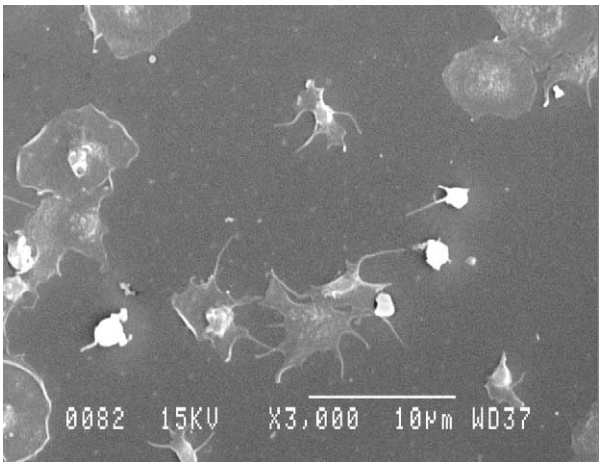

(b) a-C:H-2

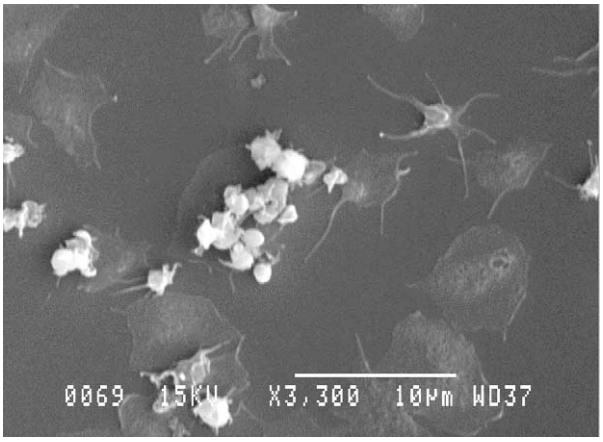

(c) a-C:H-4

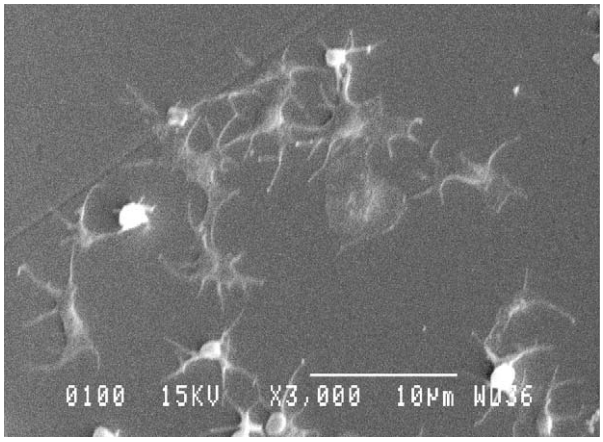

(d) Stainless steel

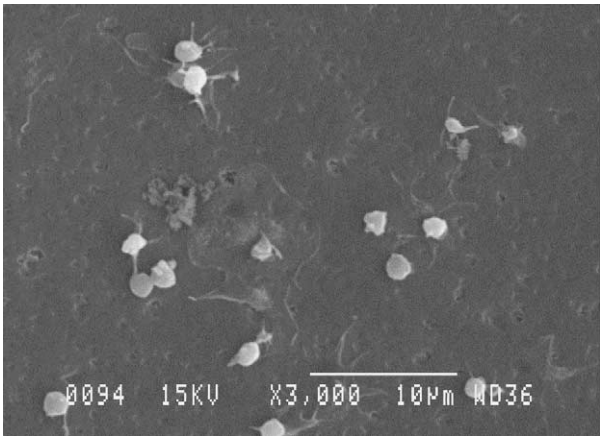

(e) LTI-carbon

Fig. 8. Morphology of adherent platelets on the a-C:H film surface (15 min incubation in PRP) observed using SEM.

3.4. Discussion on behavior of platelet adhesion and activation

The adhesion and aggregation of platelets are important steps in the process of thrombus formation. However, the way in which platelets interact with the surface is determined by the nature of the protein layer that is adsorbed on the materials surface from blood [12]. The work of adhesion (W_a) and interfacial energy (γ_{sl}) are defined as energetic parameters of the interaction between the molecules of a liquid and a solid [38]. They can be calculated from the surface tension and

Table 5
Adhesion work (W_a) and interfacial energy (γ_{sl}) of the a-C:H films—plasma protein system

Sample	$W_{a,p}$		γ_{sp}	
	Albumin	Fibrinogen	Albumin	Fibrinogen
a-C:H-1	98.58252	93.59216	10.82586	15.92084
a-C:H-2	94.78328	89.59616	12.52672	17.80474
a-C:H-4	92.75316	87.02632	15.02314	20.87028

wettability using Eq. (2) and the Young–Neuman [39] equation (Eq. (4)), respectively:

$$\gamma_{s1} = \gamma_s - \gamma_l \cos\theta. \quad (4)$$

Hence, the adhesion and interfacial energy of the two kinds of plasma protein ($W_{a,p}$ and γ_{sp}), albumin, which is known to reduce platelet adhesion [12] and fibrinogen that is an adhesive protein known to enhance the adhesion and activation of platelets [40] can be calculated. The results are listed in Table 5.

On our a-C:H films, albumin has higher W_a values than fibrinogen. The difference between the adhesion work function of the two proteins remains 5–6 mJ/m^2 and is not affected by changes of V_b. This effect indicates that albumin has slightly higher adsorption activity than fibrinogen at the interface, as manifested by the tendency of a protein to adsorb onto the surface. Jones [12] and Dion [2] found that DLC coatings exhibit a higher albumin and fibrinogen adsorption. The albumin/fibrinogen adsorption ratio was determined to be 1.008 and 1.24, respectively, in these previous studies, much higher than that of TiN, TiC and titanium. These results are consistent with our observed adsorption trend as inferred from the difference between the adhesion work functions of the two proteins. The albumin/fibrinogen adsorption ratio is important for the assessment of the adhesion of platelets onto artificial surfaces, and that the higher the ratio, the lower the number of adhering platelets. Hence, the smaller number of platelets adhered on all of the a-C:H film surfaces can be attributed to the preference of albumin adsorption.

Our results show that when the bias V_b (absolute value) is increased, the interfacial energy of albumin and fibrinogen increases from 10.8 and 15.0 to 15.9 and 20.9 mJ/m^2, respectively. It is expected because protein molecules will undergo a conformational transformation when plasma protein adsorbs onto an artificial surface (higher interfacial energy) from its aqueous phase (lower interfacial energy). Our results thus suggest that the higher the interfacial energy γ_{sp}, the larger the conformation changes. Therefore, exacerbation of activation of the platelets adhered on the a-C:H film deposited at high V_b is probably due to the changes of fibrinogen conformation.

4. Conclusion

Amorphous C:H films have been fabricated by plasma immersion ion implantation-deposition under different substrate bias voltages. The Raman, XPS and RBS results indicate that film graphitization is promoted at higher substrate bias. Our investigation of the surface energy of the films shows that the polar part of the surface energy decreases with increasing bias voltage, and the tendency is consistent with the change of the I_D/I_G ratios. It is believed that this trend is affected mainly by the reduction of the sp^3 content in the films.

Activation and the quantity of adherent platelets on the surface of the a-C:H films are influenced by the substrate bias. The higher the bias V_b, the larger is the activation of the adherent platelets. This trend is consistent with the surface energy of the films. The effects can be attributed to the preference of albumin adsorption due to the higher W_a value of albumin compared to that of fibrinogen and the changes of fibrinogen conformation caused by higher interfacial energy γ_{sp}. The blood compatibility of the a-C:H film deposited at −75 V is better than that exhibited by stainless steel and similar to that of LTI-carbon. The synthesized materials can thus be used to improve the blood compatibility of stainless steels used in blood contacting biomedical devices.

Acknowledgements

This work was jointly supported by Hong Kong CityU SRG #7001389, NSFC39870199#, State Key Basic Research #G1999064706, and High Technology Project #00-863-102-09-01 of the PRC.

References

[1] Thomson A, Law FG, Rushton N, Franks J. Biomaterials 1991;2(1):37.
[2] Dion I, Roques X, Baquey C, Baudet E, Cathalinat B, More N. Biomed Mater Eng 1993;3(1):51.
[3] Tran HS, Puc MM, Hewitt CW, Soll DB, Marra SW, Simonetti VA, Cilley JH, Del Rossi AJ. J Invest Surg 1999;12(3):133.
[4] Yamazaki K, Litwak P, Tagusari O, et al. Artif Organs 1998;22(6):466.
[5] Alanazi A, Nojiri C, Kido T, et al. Artif Organs 2000;24(8):624.
[6] Alanazi A, Nojiri C, Noguchi T, et al. ASAIO J 2000;46(4):440.
[7] Yin GF, Luo JM, Zheng CQ, et al. Thin Solid Films 1999;345:67.
[8] Jones MI, McColl IR, Grant DM, Parker KG, Parker TL. Diamond Relat Mater 1999;8:457.
[9] Yu LJ, Wang X, Wang XH, Liu XH. Surf Coat Technol 2000;128–129(1):484.
[10] De Scheerder I, Szilard M, Yanming H, et al. J Invasive Cardiol 2000;12(8):389.
[11] Gutensohn K, Baeythein C, Bau J, Fenner T, Grewe P, Koester R, Padmanaban K, Kuehnl P. Thromb Res 2000;99(6):577.

[12] Jones MI, McColl IR, Grant DM, Parker KG, Parker TL. J Biomed Mater Res 2000;52:413–21.
[13] Cui FZ, Li DJ. Surf Coat Technol 2000;131:481.
[14] Mclaughlin JA, Meenan B, Maguire P, Jamieson N. Diamond Relat Mater 1996;5:486.
[15] Courtney JM, Lamba NMK, Sundaram S, Forbes CD. Biomaterials 1994;15(10):737.
[16] Lyman DJ, Hill DW, Stirk RH, Adamson C, Mooney BR. Trans Am Soc Artif Int Organs 1972;18:19.
[17] Sunny MC, Sharma CP. J Biomater Appl 1991;6:89.
[18] Sheppard JI, McClung WG, Feuerstein IA. J Biomed Mater Res 1994;28:1175.
[19] Holland NB, Marchant RE. J Biomed Mater Res 2000;51:307.
[20] Chu PK, Qin S, Chan C, Cheung NW, Larson LA. Mater Sci Eng Rep 1996;17(6–7):207.
[21] Young T. Phil Trans R Soc (London) 1805;95:65.
[22] Van Oss CJ, Chaudhury MK, Good RJ. J Chem Rev 1988; 88:92.
[23] Robertson J. Prog Solid State Chem 1991;21:199.
[24] Robertson J, O'Reilly EP. Phys Rev B 1987;35:2946.
[25] Lopinski GP. Phys Rev Lett 1998;80:4241.
[26] Schwan J, Ulrich S, Batori V, et al. J Appl Phys 1994;80:440.
[27] Beeman D, et al. Phys Rev B 1984;30:870.
[28] Valentini L, Kenny JM, Tosi P, et al. Diamond Relat Mater 2001;10:1042.
[29] Lai KH, Chan CY, Fung MK, et al. Diamond Relat Mater 2001;10:1862.
[30] Li DJ, Cui FZ, Gu HQ. Appl Surf Sci 1999;137:31.
[31] Merel P, Tabbal M, Chaker M, Moisa S, Margot J. Appl Surf Sci 1998;136:105.
[32] Haut R, Muller U, Francz G, et al. Thin Solid Films 1997;308:191.
[33] Knight DS, White WB. J Mater Res 1989;4(2):385.
[34] Dollish FR, Fateley WG, Bentley FF. Characteristic Raman frequencies of organic compounds. New York: Wiley, 1974.
[35] Colthup NB, Daly LH, Wiberly SE. Introduction to infrared and Raman spectroscopy, 3rd ed. New York: Academic Press, 1990.
[36] Pinzari F, Ascarelli P, Cappelli E, Mattei G, Giorgi R. Diamond Relat Mater 2000;10:781.
[37] Goodman SL, Tweden SK, Albrecht RM. J Biomed Mater Res 1996;32:249.
[38] Novikov NV, Khandozhko SI, Perevertailo VM, et al. Diamond Relat Mater 1998;7:1263.
[39] Adamson AW. Physical chemistry of surface. New York: Interscience Publishers, 1960. p. 747.
[40] Elam JH, Nygren H. Biomaterials 1992;13(1):3.